

Effect of dopants(Tri-valent, Penta-valent) on the electrical and optical properties of SnO₂ based transparent electrodes

G. W. Kim^a, C. H. Sung^a, Y. J. Seo^a, K. Y. Park^a, S. N. Heo^a, S. H. Lee^b and B. H. Koo^{a,*}

^aSchool of Nano & Advanced Materials Engineering, Changwon National University, Changwon 641-773, Gyeongnam, Korea

^bDepartment of Material Processing, Advanced Thin Film Research Group, Korea Institute of Materials Science (KIMS), Changwon 641-010, Gyeongnam, Korea

In this work, we studied the influence of the dopant elements concentration on the properties of SnO₂ thin films deposited by pulsed laser deposition. X-ray diffraction (XRD), field emission scanning electron microscopy (FE-SEM), Hall effect measurement and UV-Vis studies were performed to characterize the deposited films. XRD results showed that the films had polycrystalline nature with tetragonal rutile structure. FE-SEM micrographs revealed that the as deposited films composed of dense microstructures with uniform grain size distribution. All the films show n-type conduction and the best transparent conductive oxide (TCO) performance was obtained on 6 wt% Sb₂O₅ doped SnO₂ film prepared at pO₂ of 60mtorr and Ts of 500 °C. Its resistivity, optical transmittance, figure of merit are $7.8 \times 10^{-4} \Omega \text{ cm}$, 85% and $1.2 \times 10^{-2} \Omega^{-1}$, respectively.

Key words: Transparent Conductive Oxide (TCO), Transmittance, Tin Oxide(SnO₂), Figure of merit.

Introduction

Transparent conducting oxides (TCOs) have wide range of application areas in transparent electrode for display devices, transparent coating for solar energy heat mirrors, solar cells and gas sensors [1-4]. It is well known that widely-used TCO thin films such as ZnO, SnO₂, ITO are n-type because of the existence of intrinsic defects (oxygen vacancies and/or metal interstitials). As compared with indium tin oxide (ITO) which is more widely used, SnO₂ films are inexpensive, chemically stable in acidic and basic solutions, thermally stable in oxidizing environments at high temperature, and also mechanically hard [5]. Various deposition methods have been employed for the preparation of TCO films. Among them, pulsed laser deposition (PLD) has attracted much attention because the fabrication process is quite suitable for optoelectronic devices using the SnO₂ as a transparent electrode [6-8] Furthermore, the composition of films grown by PLD is quite close to that of the target, and it is true even for a multi component target.

In this study, transparent conducting SnO₂ films with various dopant (tri-valent, penta-valent) contents, and thickness were deposited by pulsed laser deposition process at a fixed oxygen pressure (60 mtorr) and substrate temperature (500 °C) on the glass substrates. The structural properties of electrodes were studied by observing the X-ray diffraction (XRD) patterns and the

morphology was analyzed by using field emission scanning electron microscope (FE-SEM) images. The optical properties of films were studied by the UV-visible transmittance. The electrical properties were investigated by the Hall measurements. Figure of merit were computed from spectral transmittance and film thickness dependent resistivity data.

Experimental

The SnO₂ : dopants (tri-valent, penta-valent) films were deposited on the glass substrates by PLD technique. A sintered doped SnO₂ ceramic target was prepared by the solid state reaction method. The stoichiometric amount of highly pure SnO₂ (99.99%) and dopants (99.9% purity) powders were mixed. The contents of the dopant added to the used target was 0 ~ 10 wt%. Finally, the samples were ground to fine powder, pressed into pellet form, and sintered at 1250 °C for 12 hrs followed by slow cooling (at 4 °C/min). During the deposition, laser energy density at the target surface was kept at 2 J/cm² and laser frequency at 2 Hz. The focused laser beam was incident on the target surface at an angle of 45 °. The target was rotated about 10 rpm and the substrate was mounted opposite to the target at a distance of 45 mm. After the deposition, the thin films were cooled down slowly to the room temperature at a rate of 5 °C/min. The film thickness was measured by a stylus profilometer. The structural properties of the films were analyzed by X-ray diffraction (XRD, Cu K α 1, $\lambda = 0.154 \text{ nm}$) and the scans were performed with 0.02 ° step size in the 2 θ range of 20-80 °. Morphology of the deposited films

*Corresponding author:
Tel : +82 55 264 5431
Fax: +82 55 262 6486
E-mail: bhkoo@changwon.ac.kr

was analyzed by field emission scanning electron microscopy (FE-SEM; MIRA II, Tescan). Electrical properties were checked by a four-point probe sheet resistance (Mitsubishi Loresta MCP-T610 TFP probe) and Hall measurement. The optical properties of the films were studied at room temperature with a UV-VIS-NIR spectrometer in the wavelength range of 300-800 nm. The figure of merit is calculated on the optical transmittance for the range of 400-800 nm and the sheet resistance R_s .

Results and discussion

In order to find the effect of doping element, we have studied the resistivity with using various doping elements in SnO₂. The variation in the resistivity of tri-valent and penta-valent elements doped SnO₂ films at 500 °C as a function of concentration (0 ~ 10 wt%) is shown in Fig. 1(a-b). It is clear that the resistivity of the SnO₂ films doped with all the trivalent elements such as Bi₂O₃, Al₂O₃, Y₂O₃, Ga₂O₃ and Sb₂O₃ first decrease and then increase with the increase of dopant concentration. Interestingly, 6 wt% Bi₂O₃ doped SnO₂ film shows higher resistivity, while 6 wt% Sb₂O₃ doped SnO₂ film shows lower value of resistivity. In the case of pentavalent elements such as Nb₂O₅, Ta₂O₅ and Sb₂O₅ doped SnO₂ films (Fig. 1(b)), similar decreasing

and increasing trend of resistivity with the increase of dopant content was observed. The lower value of resistivity was observed for 6wt% Sb₂O₅ doped SnO₂ film, while 6 wt% Nb₂O₅ doped SnO₂ film showed higher value of resistivity. Doping with Sb₂O₃ and Sb₂O₅, the SnO₂ films have significantly decreased in resistivity. The decrease in resistivity is due to the substitution of Sn by Sb as their ionic radii are matching [9]. It is observed that this substitution increases the carrier concentration and thereby decreases resistivity. In comparison with Sb₂O₃ to Sb₂O₅, we observed the lowest value of resistivity of $7.84 \times 10^{-4} \Omega \text{ cm}$ for the doping of 6 wt.% Sb₂O₅ at 500 °C substrate temperature. This is due to the substitutional incorporation of Sb⁵⁺ ions at Sn⁴⁺ cation sites or incorporation of Sb ions in interstitial positions. The excess Sb doping introduces Sb³⁺ ions, which act like acceptors that compensate for the donor levels created by the Sb⁵⁺ ions. Thus, the excess Sb doping decreases the carrier concentration in the film and consequently increases the resistivity [10].

The electrical properties of SnO₂ : Sb films strongly depends on the parameters such as Sb₂O₅ content, substrate temperatures, film thickness and oxygen partial pressures. The electrical resistivity (ρ), carrier concentration (n), and Hall mobility (μ) of the films were measured at room temperature using the four probe point method. Fig. 2 shows the variation of the electronic transport parameters (ρ , n , μ) of SnO₂ : Sb films with Sb₂O₅ content in the targets used for deposition. The carrier concentration gradually increases until 4 wt.% of Sb₂O₅ content because of the substitution of Sb⁴⁺ by Sn⁴⁺ as their ionic radii are matching (Sn⁴⁺ 0.071 and Sb⁵⁺ 0.065 nm) or incorporation of Sb⁵⁺ cations in interstitial position and then above 4 wt.%, the saturation in the carrier concentration occurred. The value of resistivity decreased from doping level of 0 to 6 wt.% due to the increase in free carrier concentrations as a result of the donor electrons from the dopant (Sb). This result is similar to the earlier reported results on the doped SnO₂ films [11]. However, it is indicating

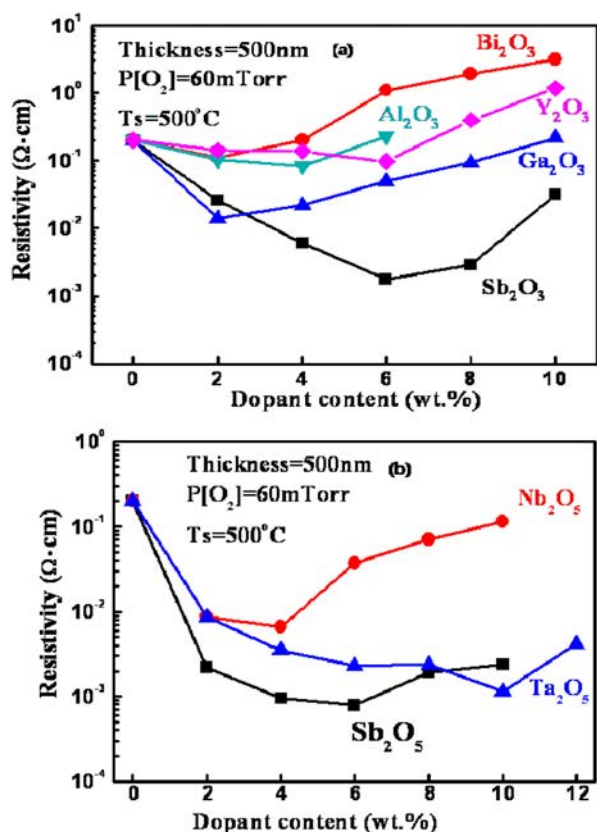


Fig. 1. Variation of electrical resistivity as a function of (a) tri-valent doped SnO₂ thin films with different doping level and (b) penta-valent doped SnO₂ thin films with different doping level.

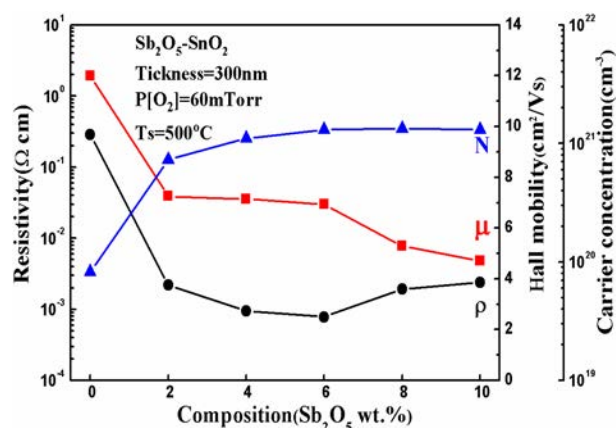


Fig. 2. Resistivity (ρ), mobility (μ) and carrier concentration (n) as a function of composition for Sb₂O₅ doped SnO₂ thin films.

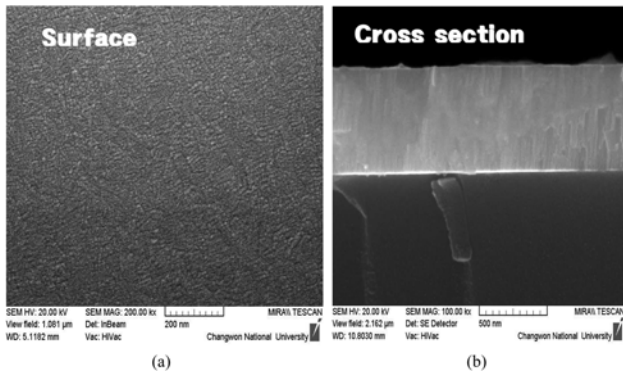


Fig. 3. FE-SEM image (a) in planer and (b) cross-sectional view for Sb-doped SnO₂ film (6 wt % of Sb content) deposited at substrate temperature of 500 °C.

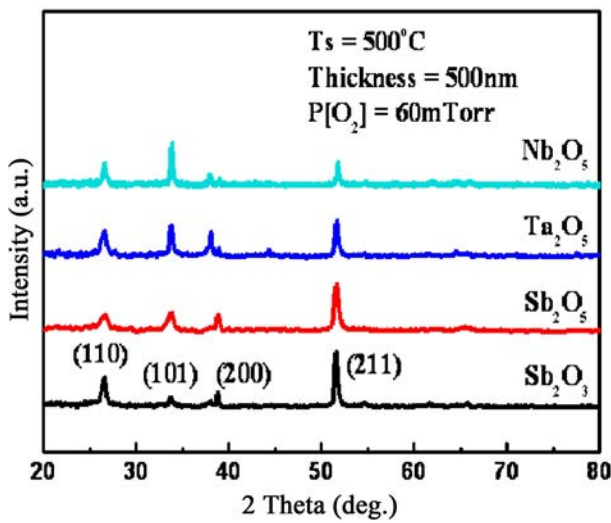


Fig. 4. XRD patterns of the SnO₂ thin films deposited at 500 °C as a function of doping elements.

that Hall mobility decreasing with increasing Sb content caused by grain boundary scattering and ionized impurity scattering. Therefore, at a 6 wt. % of Sb content, the resistivity reached the lowest value and then increased with a further increase of Sb content.

Fig. 3 displays the surface and the cross-sectional FE-SEM images of the Sb-doped SnO₂ (6 wt% of Sb content) film deposited on the glass substrate. The Film was deposited at a substrate temperature of 500 °C. Fig. 3(a) shows that the film possesses a uniform grain-size distribution with dense microstructures. The cross-sectional view of the film also reveals the dense microstructure as shown in Fig. 3(b).

Fig. 4 shows the XRD patterns of SnO₂ thin films doped with tri-valent and penta-valent elements. The XRD patten of the SnO₂ powders is indexed to the tetragonal rutile structure with lattice constants of a = 0.473 nm and c = 0.318 nm from JCPDS card (41-1444). Although some secondary phase such as Sn₃O₄ and SnO could be contained [12], however, the samples in this study had no secondary phases. The XRD patterns of the SnO₂ films are identical to that of

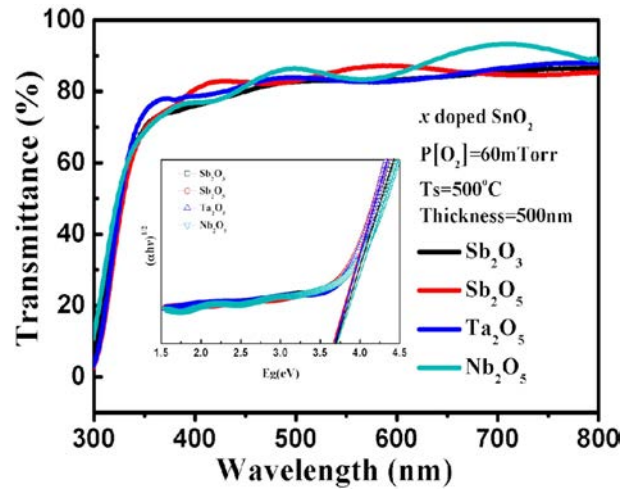


Fig. 5. (a) The optical transmittance spectra of SnO₂ thin films with different doping elements and (b) The Tauc plots ($n = 1/2$) of SnO₂ thin films with different doping elements.

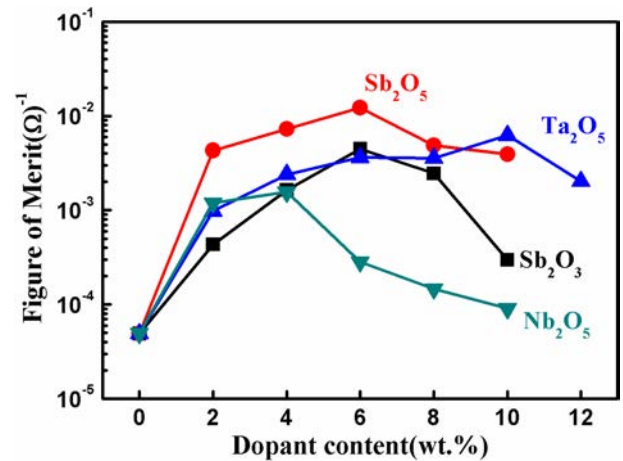


Fig. 6. Variation of figure of merit for the different doping elements. SnO₂ thin films deposited with different deposition dopant content.

the SnO₂ powders, indicating that these films are indeed SnO₂. All the films show a polycrystalline nature with orientations along [110], [101], [200] and [211] planes.

Fig. 5 shows the transmittance spectra of the films deposited at 500 °C and 60 m Torr of oxygen pressure with different dopants in the visible region (300 nm ~ 800 nm). The average transmittance in the visible region was observed between 86% and 83%. Consequently, all the films exhibited high transparency in the visible region. The optical band gap of the films was derived from the plots (inset of Fig. 5) of $(\alpha h\nu)^{1/2}$ vs $h\nu$, where α is the absorption coefficient and $h\nu$ is photon energy. It was observed that optical band gap slightly increase from 3.65 to 3.67 eV. This increase in band gap is attributed to slight increases in the crystallinity of the films.

The figure of merit is a significant factor for estimating TCO thin films in relation to their applications. Conductivity and transmittance are inversely proportional

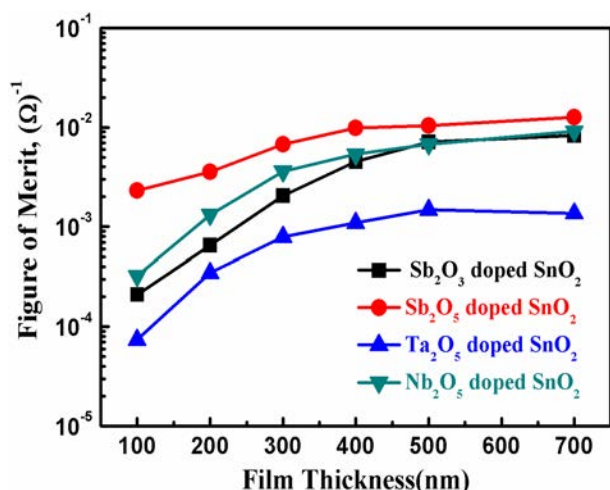


Fig. 7. The figure of merit of the different elements doped SnO₂ thin films as functions of films thickness.

to each other and should be as high as possible for effective usage. The figure of merit is widely used to compare the performance of various transparent conductors as first defined by Haacke [13] is, $\Phi = Tr/10/R_s$ where Tr is the optical transmittance for the range of 400-800 nm and R_s is the sheet resistance. In Fig. 6, the effect of dopant elements and concentration in the figure of merit is observed. The maximum value of figure of merit (ΦTC) is observed to be $12.6 \times 10^{-3} \Omega/cm$ for the SnO₂:Sb₂O₅ films deposited with 6% dopant content. This value is higher than the SnO : Sb thin film obtained from previously reported paper [11].

Fig. 7 show a plot of the figure of merit vs. deposition thickness of the different elements doped SnO₂. The figure of merit increases consistently with the increase in films thickness. This can be explained as follows: usually in thin films the resistivity depends on the film thickness. In bulk, the resistance to the charge carrier is usually caused by photon scattering, impurity and defect scattering. In the case of thin film, there is an additional scattering from the surface. [14] We can therefore conclude that Sb₂O₅ doped SnO₂ thin film having very low resistivity and high transparency may be used as an alternative for transparent conductive electrodes.

Conclusions

In summary, high quality transparent conducting SnO₂ : Sb films have been successfully grown on the glass substrates by PLD technique. The structural, electrical and optical properties of the SnO₂ : Sb films

were investigated as a function of doping level and film thickness at fixed substrate deposition temperature and oxygen pressure. For a 300 nm SnO₂ : Sb film deposited at $T_s = 500^\circ C$ and 60 mtorr of oxygen pressure, an electrical resistivity of $7 \times 10^{-4} \Omega \cdot cm$ with an average optical transmittance of 84% in the visible range (400 ~ 800 nm) was observed. The maximum value of figure of merit (ΦTC) was observed $12.6 \times 10^{-3} \Omega/cm$ for the SnO₂ : Sb₂O₅ films. This study shows the ability to grow SnO₂ : Sb films with low resistivity, high optical transmission and high figure of merit by PLD method. This is important for the fabrication of high quality transparent electrodes

Acknowledgements

This research was supported by the MKE (The Ministry of Knowledge Economy), Korea, under the ITRC (Information Technology Research Center) support program supervised by the NIPA (National IT Industry Promotion Agency) (NIPA-2012-H0301-12-2009).

This research was financially supported by the Ministry of Education, Science Technology (MEST) and National Research Foundation of Korea (NRF) through the Human Resource Training Project for Regional Innovation (2012H1B8A2026212).

References

1. Y.S. He, J.C. Campbell, R.C. Murphy, M.F. Arendt, J.S. Swinnea, *J. Mater. Res.* 8 (1993) 3131.
2. W.A. Badway, H.H. Afifi, E.M. Elgai, *J. Electrochem.soc.* 137 (1990) 1592.
3. Y.L. Fang, J.J. Lee, *Thin Solid Films.* 169 (1989) 52.
4. J.C. Manificier, L. Szepessy, J. F. Bresse, M. Perotin, R. Stuck, *Mater. Res. Bull.* 14 (1979) 109.
5. H. Kim, R. C. Y. Auyeung, A. Pique, *Thin Solid Films.* 516 (2005) 5052.
6. H. Kim, A. Pique, J.S. Horwitz, H. Mattoussi, H. Murata, Z.H. Kafafi, D.V. Chrisey, *Appl. Phys. Lett.* 74 (1999) 3444.
7. Y. Onuma, Z. Wang, H. Ito, N.M. Nakato, K. Kamimura, *Jpn. J. Appl. Phys. Part I* 37 (1998) 963.
8. H. Kim, J.S. Horwitz, G. Kushito, Z.H. Kafafi, and D.B. Chrisey, *Appl. Phys. Lett.* 79 (2001) 284.
9. R.D. Shannon, *Acta Cryst.* A32 (1976) 751.
10. B.Thangaraju, *Thin Solid Films* 402 (2002) 71.
11. S. Shanthi, C. Subramaniam, P. Ramasamy, *J. Crystal Growth.* 197 (1999) 858.
12. N. s. Murty, S. R. Jawalekar, *Thin Solid Films.* 108 (1983) 277.
13. G. Haacke, *J. Appl. Phys.* 47 (1976) 4086-4089.
14. A.M. Bazargan, S.M.A. Fatemina, M. Esmailpour Ganji, M.A. Bahrevar, *Chem .Eng. J.* 155 (2009) 523.